Applied Nanoscience (2018) 8:675–683
https://doi.org/10.1007/s13204-018-0698-8

ORIGINAL ARTICLE

Structural characterization of mesoporous magnetite nanoparticles synthesized using the leaf extract of *Calliandra haematocephala* and their photocatalytic degradation of malachite green dye

Karthikey Devadatta Sirdeshpande[1] · Anushka Sridhar[1] · Kedar Mohan Cholkar[1] · Raja Selvaraj[1]

Received: 18 November 2017 / Accepted: 21 February 2018 / Published online: 1 March 2018

Abstract
A simple method for the synthesis of magnetite nanoparticles using the leaf extract of *Calliandra haematocephala* has been developed. UV–Vis spectrum showed a characteristic strong absorption band. SEM image revealed the bead-like spherical nanoparticles. EDS showed the prominent peaks for elemental iron and oxygen. PXRD patterns confirmed the crystalline nature and the average crystallite size of 7.45 nm. In addition, the lattice parameter value was calculated to be 8.413 Å, close to Fe_3O_4 nanoparticles. BET analysis disclosed the total specific surface area of the nanoparticles as 63.89 m^2/g and the mesoporous structure of the nanoparticles with a pore radius of 34.18 Å. FTIR studies showed the specific bands at 599.82 and 472.53 cm^{-1}, typical for Fe_3O_4 nanoparticles. The photocatalytic efficacy of the nanoparticles was demonstrated against the degradation of malachite green dye under sunlight irradiation and the photocatalytic degradation constant was calculated as 0.0621 min^{-1}.

Keywords *Calliandra haematocephala* · Magnetite nanoparticles · Green synthesis · Dye degradation · Mesoporous nanoparticles · BET analysis

Introduction

Nanoparticles are individual complexes or clusters that are 100 nm in size or less. Their smaller size gives them a unique edge over other particles that are of micrometer size. Magnetite (Fe_3O_4) nanoparticles, a common iron oxide, has numerous applications in various fields because of their inherent physico-chemical features. For instance, magnetite nanoparticles have been extensively used in the biomedical field for cancer therapy, drug delivery, cellular labeling and tissue repair (Siddiqi et al. 2016), in biotechnology as antimicrobial and antioxidant agents (Muthukumar and Iswarya 2017), for immobilization of enzymes (Kumari and Singh 2016), in environmental applications for the removal of hazardous dyes, heavy metals (Ibrahim et al. 2016), pesticides (Guo et al. 2017) and the development of pesticide detection sensor (Chauhan et al. 2015).

Traditionally, the magnetite nanoparticles are synthesized by reacting an iron salt ($FeCl_3$, $FeCl_2$, $Fe(NO_3)_3$ or $FeSO_4$) and sodium borohydride with specific quantities. Nevertheless, this method suffers due to the high process cost and the toxic nature of borate salt production which lead to environmental pollution. There are few modified procedures available in the literature such as using surfactants (Nabiyouni et al. 2015) and ultrasonication (Ghanbari et al. 2014) for the synthesis which increase the total cost. Very recently, an article (Ren et al. 2017) has described a modified chemical procedure, but has the limitation of low specific surface area (only 10.6 m^2/g) of the magnetite nanoparticles.

Therefore, the development of a low cost, non-toxic and simple method with exceptional physico-chemical properties of magnetite nanoparticles is the need of the hour. Synthesis of nanoparticles by using the polyphenols extracted from various plant parts by "green synthesis", commonly known as "plant-extract mediated green synthesis" (PMGS) can be an alternative to the traditional chemical and physical methods. As reported in an article (Peralta-videa et al. 2016), there has been a constant increase in the articles based on

✉ Raja Selvaraj
rajaselvaraj@gmail.com

[1] Department of Biotechnology, Manipal Institute of Technology (MIT), Manipal Academy of Higher Education, Manipal, Karnataka 576104, India

PMGS of nanoparticles since 2006 and depicted an exponential enhancement.

Polyphenols are present in all the plants as secondary metabolites. The basic principle behind the PMGS is the reducing potential of the polyphenols residing in the plant parts. Many reports (Smuleac et al. 2011; Huang et al. 2015; Huang et al. 2014; Hoag et al. 2009) indicate that the higher reduction potential of polyphenols is sufficient for the reduction of metallic salts to form nanoparticles. In addition to the reduction, the polyphenols cap the nanoparticles thereby provide them stability and minimize the aggregation. This feature eliminates the addition of separate stabilizing agent during nanoparticle synthesis (Litvin and Minaev 2013), (Litvin and Minaev 2014). It is needless to mention here that the polyphenols are environmentally benign and are biodegradable.

It is shown by many researchers that Fe_3O_4 nanoparticles can be synthesized using various plant extracts. For example, Andean blackberry leaf extract (Kumar et al. 2016), *Pisum sativum* peel extract (Prasad et al. 2017), *Syzygium cumini* seed extract (Venkateswarlu et al. 2014a), plantain peel extract (Venkateswarlu et al. 2013), *Punica Granatum* rind extract (Venkateswarlu et al. 2014b) have been successfully utilized for the synthesis of Fe_3O_4 NPs. Various agro-waste extracts have been used for the synthesis of Fe_3O_4 nanoparticles recently (Stan et al. 2017).

Motivated by these recent studies, in the present investigation, we made an attempt to synthesize Fe_3O_4 nanoparticles using the leaf extract of *Calliandra haematocephala*. Our research group was the first one to demonstrate the reduction potential of the polyphenols present in this leaf extract for the synthesis of silver nanoparticles (Raja et al. 2017).

It is well known that the iron oxide nanoparticles have renowned photocatalytic activity by the virtue of their low band gap, more stableness, high surface area and good light absorption capacity (Muthukumar and Matheswaran 2015) (Zazouli et al. 2017; Xu et al. 2014; Wang et al. 2017; Gupta et al. 2017). Therefore, the objectives of the present study are threefold: (1) synthesis of Fe_3O_4 nanoparticles using the leaf extract of *Calliandra haematocephala,* (2) characterization of the nanoparticles and (3) photocatalytic degradation of a pollutant dye, Malachite Green (MG) under sunlight irradiation.

Materials and methods

Materials

Analytical grade chemicals were used for all the experiments. $FeSO_4{\cdot}7H_2O$, NaOH, HCl and malachite green (MG) dye were purchased from Merck, India.

Preparation of the leaf extract of *Calliandra haematocephala*

The leaf extract was prepared according to the procedure given in our earlier report (Raja et al. 2017). Briefly, the leaves from the plant, *Calliandra haematocephala,* were collected. They were initially washed with tap water to remove the dust particles settled on the surface and subsequently with double-distilled water. The thoroughly washed leaves were then air-dried for about an hour. About 50 g of the dried-leaves was added to 500 mL of double-distilled water in a beaker. The contents were heated for 30 min for the release of phenolic compounds which was indicated by the appearance of brown color. The beaker was cooled under running tap water and the contents were filtered. The brown color filtrate thus obtained was named as *Calliandra haematocephala* leaf extract (CHLE) which was stored at 4 °C until further use.

Synthesis of magnetic Fe_3O_4 nanoparticles

In a glass beaker, a freshly prepared 0.1 M $FeSO_4$ solution was added to CHLE at a volume ratio of 1:1 at room temperature. Upon addition, the mixture instantly turned greenish-black in color which indicated the incipient formation of colloidal nanoparticles. The pH of this mixture was increased to 11 by adding the previously prepared 2 N NaOH. The mixture was then placed in a water bath for 60 min at 90 °C. The intense black precipitate indicated the synthesis of magnetic Fe_3O_4 nanoparticles (CH–Fe_3O_4NPs). The formed nanoparticles were isolated by applying a strong magnet and washed several times with water and then with ethanol. The purified NPs were dried in a hot air oven for 4 h at 120 °C and stored in an airtight container for further characterization and usage.

Characterization

The synthesis and photocatalytic activity of the CH–Fe_3O_4NPs were monitored from the absorbance spectra taken using a UV–visible, double-beam spectrophotometer (SHIMADZU—UV1700). A diluted colloidal suspension was used to record the spectrum of nanoparticles. Similarly, a thin film of colloidal suspension on a glass slide was used for recording the images using Scanning Electron Microscope (EVO MA18). The elemental composition was analyzed by Energy-dispersive X-ray analysis (OXFORD). The powder X-ray diffraction (PXRD) patterns were obtained by employing Rigaku Miniflex 600 X-Ray diffractometer to study the crystalline structure. FTIR measurements were made with a

SHIMADZU-8400S spectrophotometer using KBr pellet method. The total specific surface area (SSA_T) and the total pore volume (V_P) of the CH–Fe_3O_4NPs were determined from nitrogen adsorption–desorption isotherms obtained by BET apparatus (Smart Instruments, Mumbai).

Photocatalytic degradation of malachite green dye

The photocatalytic degradation of MG dye was studied by exposing a mixture of known concentration (20 ppm) of MG dye solution and 100 mg of the CH–Fe_3O_4NPs in a glass beaker under sunlight. A control experiment (without nanoparticles) was also performed. The progress of the photocatalytic degradation was visually and spectrophotometrically monitored at periodic time intervals. The reduction in the absorption maximum at a wavelength of 617 nm was the indication of dye degradation. The residual concentration of the dye was calculated from a calibration plot.

Results and discussion

Visual inspection

The synthesis of nanoparticles was first visually inspected with respect to the color change of the reaction mixture. The addition of $FeSO_4$ (Fig. 1a) to the CHLE (Fig. 1b) immediately formed a greenish-black colloidal suspension. This signaled the synthesis of nanoparticles. However, the as-synthesized nanoparticles did not have any magnetic property. Therefore, the pH of the contents was increased to 11 and upon heating for 60 min at 90 °C (Kumar et al. 2016) yielded an intense black color magnetic CH–Fe_3O_4NPs nanoparticles (Fig. 1c). The magnetic behavior of the nanoparticles is depicted in Fig. 1d.

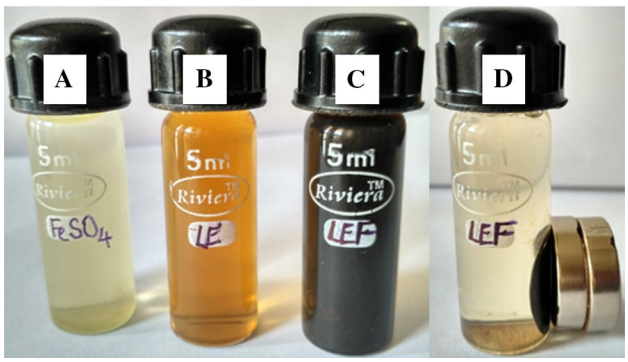

Fig. 1 Photographs of the vials containing $FeSO_4$ (**a**), CHLE (**b**), CH–Fe_3O_4NPs (**c**) and magnetic attraction of CH–Fe_3O_4NPs (**d**)

UV–Vis study

The CHLE is known to contain many phytochemicals such as gallic acid, caffeic acid and quercitrin, etc., as mentioned in our earlier study (Raja et al. 2017). The literature reveals that these phytochemicals first form complexes with the iron salts and then reduce the ions to form nanoparticles (Hoag et al. 2009). The reduction is feasible and spontaneous since the standard reduction potential of polyphenols is between 0.3 and 0.8 V, whereas for the Fe, it is only − 0.44 V (Huang et al. 2014). The UV–vis spectrum of synthesized nanoparticles after multi-folded dilution is shown in Fig. 2. A continuous absorption band was observed without any specific peak in the entire spectrum, which is typical for iron-based nanoparticles. Similar type of UV–vis spectrum was shown for the magnetite nanoparticles synthesized using Andean blackberry leaf extract (Kumar et al. 2016). The results obtained in the present study are in good agreement with published reports (Devatha et al. 2016; Irshad et al. 2017; Mahdavi et al. 2013).

SEM and EDS

The morphology of the purified nanoparticles using the CHLE was analyzed using SEM image (Fig. 3). A bead-like, spherical nanoparticle with slight aggregation can be seen. Two of such nanoparticles, 85.41 and 87.89 nm, are mentioned in the Fig. The aggregate formation may be due to the magnetic property of the nanoparticles. In order to minimize the surface energies, the NPs tend to aggregate (Balamurugan 2014). This type of aggregates has been documented earlier for the green synthesis of nanoparticles (Kumar et al. 2016; Devatha et al. 2016).

To study the elemental composition of CH–Fe_3O_4NPs, EDS was performed (Fig. 4). The results from the EDS showed the prominent peaks for elemental iron and oxygen, which ascertained the formation of the iron oxide nanoparticles. The weak peak for silicon presumably arose from the glass slide which held the thin film of sample (Mubarakali et al. 2011). The presence of carbon peak probably originated from the polyphenol groups, inherent to the leaf extract (Wang et al. 2014). This also corroborated the fact of capping action of polyphenols on the surface of the CH–Fe_3O_4NPs.

As mentioned in the inset of the Fig. 4, the composition of each element in the sample (weight %) was as follows: Fe–56.50, O–38.71, C–3.58 and Si–1.20. The higher concentration of Fe and O confirmed the synthesis of iron oxide nanoparticles. Similar kind of results has been reported by other investigators (Devatha et al. 2016; Belachew et al. 2016; Wang et al. 2014) for the green synthesis of nanoparticles.

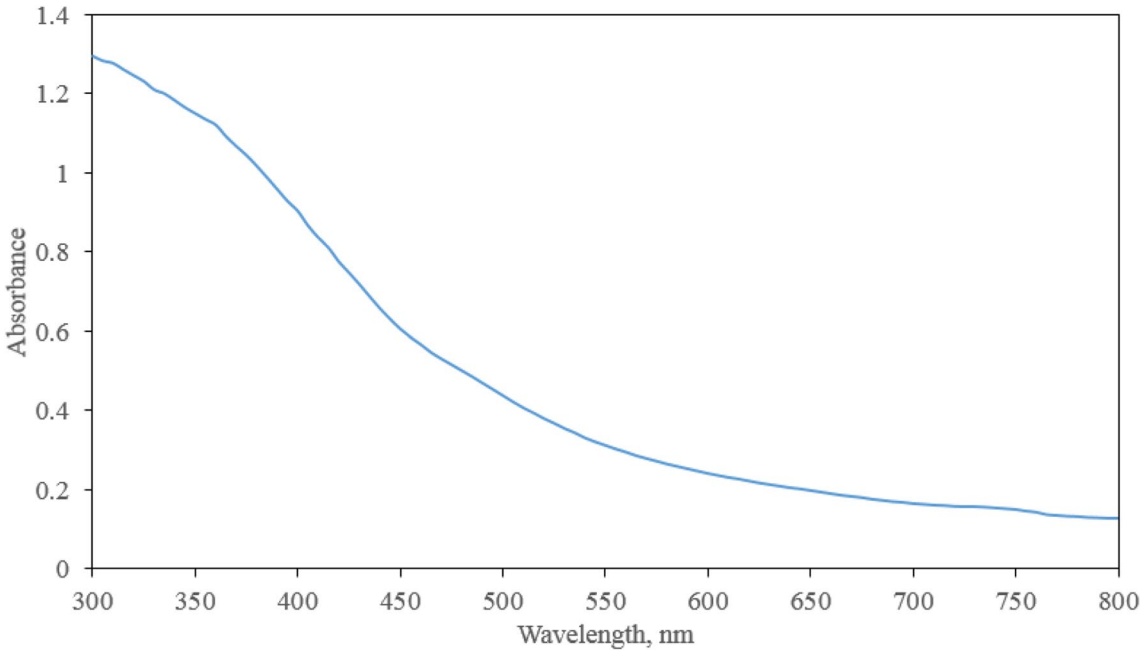

Fig. 2 UV–Vis spectra of the CH–Fe_3O_4NPs

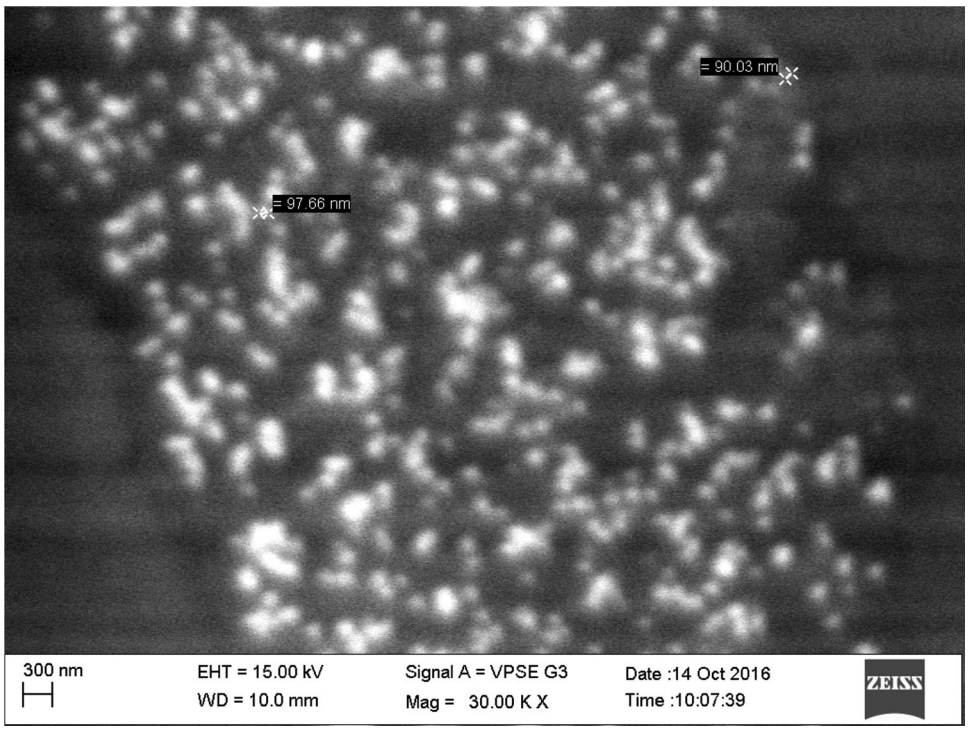

Fig. 3 SEM image of the CH–Fe_3O_4NPs

XRD

Figure 5 shows the PXRD patterns of the purified CH–Fe_3O_4NPs. Two distinctive peaks for NPs at 2θ of 35.42° and 63.02° were observed which were assigned to (311) and (440) indices, respectively. These peaks and indices are consistent with the cubic inverse spinel structure of magnetite in the standard JCPDS file No. 19-0629. The absence of other peaks such as $FeSO_4$, FeOOH or Fe_2O_3 substantiated the purity of the CH–Fe_3O_4NPs and confirmed the synthesis of magnetite nanoparticles (Kumar et al. 2016), (Darroudi et al. 2014), (Gholoobi et al. 2017).

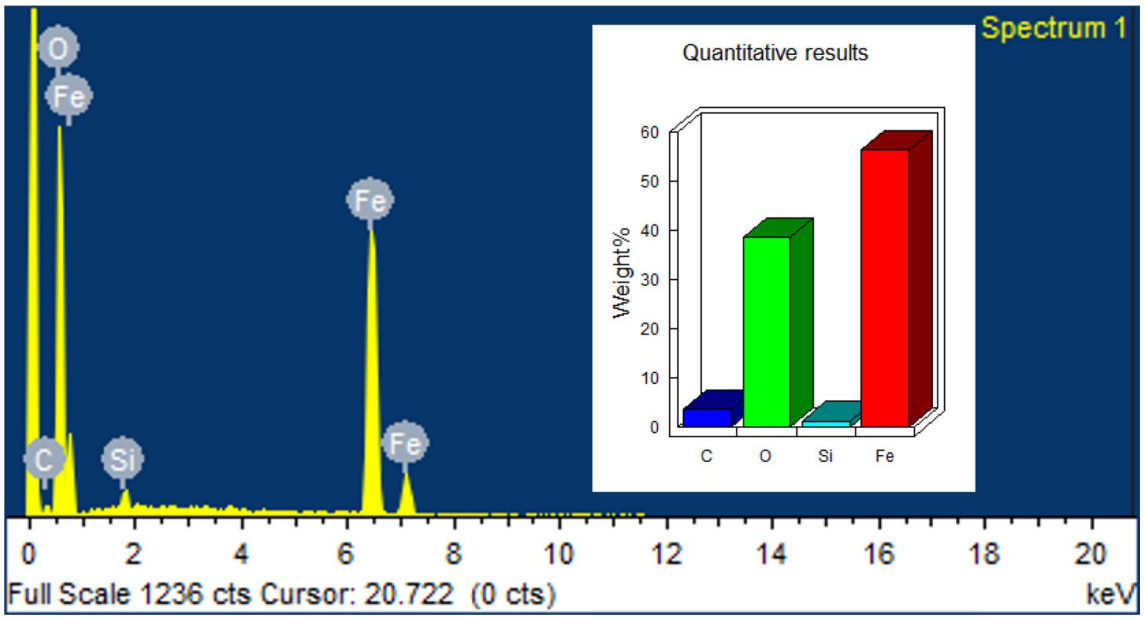

Fig. 4 EDS spectrum of the CH–Fe_3O_4NPs

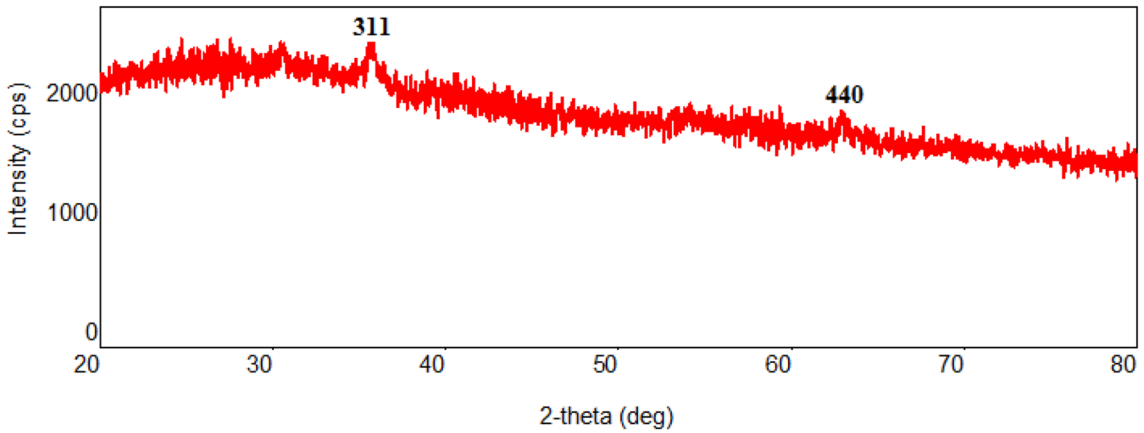

Fig. 5 XRD pattern of the CH–Fe_3O_4NPs

The highest intensity plane, i.e. (311) was considered for the calculation of crystallite size using the Debye–Scherrer formula (Gholoobi et al. 2017) and a crystallite size of 17.28 nm was obtained. A study conducted by a research group (Belachew et al. 2016) reported an average crystallite size of 10.5 nm for the L-Met capped Fe_3O_4 nanoparticles. Likewise, an average size of 10 ± 3 nm has been mentioned for the synthesis of supramagnetic Fe_3O_4 nanoparticles with maltose as the reducing agent (Demir et al. 2013).

A d-spacing value of 2.53 Å and a lattice parameter (a) of 8.399 Å for the Miller indices corresponding to (311) plane endorsed the standard values for magnetite (El Ghandoor et al. 2012). This is in agreement with the lattice parameter value of 8.386 Å, reported for the synthesis of magnetic Fe_3O_4 nanoparticles using plantain peel extract (Venkateswarlu et al. 2013).

BET analysis

Table 1 depicts the comparison of the total specific surface area (SSA_T) and total pore volume (V_P) of green synthesized Fe_3O_4 nanoparticles using various green sources. In the current study, the SSA_T and V_P of the CH–Fe_3O_4NPs were determined as 63.89 m^2/g and 0.1092 cm^3/g, respectively, by the nitrogen adsorption–desorption isotherms based on BET model. It is clear from the Table 1 that the Fe_3O_4 synthesized by our method has the highest specific surface area and may find applications in the development

Table 1 Comparison of the total specific surface area (SSA_T) and total pore volume (V_P) of the green synthesized Fe_3O_4 nanoparticles using various plant sources

S. No.	Source	SSA_T (m^2/g)	V_P (cm^3/g)	References
1.	*Syzygium cumini* seed extract	3.517	0.9905	Venkateswarlu et al. (2014a)
2.	*Punica Granatum* rind extract	10.88	0.07063	Venkateswarlu et al. (2014b)
3.	Plantain peel extract	11.31	0.040809	Venkateswarlu et al. (2013)
4.	*Pisum sativum* peel extract	17.60	–	Prasad et al. (2017)
5.	*Ridge gourd* peel extract	26.21	0.134	Cheera et al. (2016)
6.	*Calliandra haematocephala* leaf extract	63.89	0.1092	This study

of novel catalysts. The cylindrical pore radius was calculated as 34.18 Å which authenticated the mesoporous structure of Fe_3O_4 (Huang and Tang 2005). It is reported that the larger surface area and mesoporous structure of the nanoparticles make them a valuable candidate in many fields (Shaofeng et al. 2011). The particle size was calculated as 18.78 nm by using the procedures given in the following articles (Taha and Ibrahim 2014) (Mascolo et al. 2013).

FTIR analysis

The FITR spectrum (Fig. 6) was used to identify the possible biomolecules present in the CHLE responsible for the reduction and capping of the CH–Fe_3O_4NPs. The comparison of the FTIR data of NPs with standard absorption bands is shown in the Table 2.

As represented in the Table 2, the bands at 3645, 3550 and 2935 cm^{-1} correspond to the O–H stretching vibration of polyphenolic compounds. The sharp band at 1662 and 1610 cm^{-1} are related to the C=C stretching and N—H bending vibrations of alkenes and amide groups of proteins. The C–O stretching vibrations are attributed to the multiple bands shown at 1280, 1024 and 1122 cm^{-1}.

The bands between 400 and 600 cm^{-1} can be related to the Fe–O stretching vibrations. In the present study, bands at 599 and 472 cm^{-1} were observed, which correspond to characteristic Fe–O bond and indicated the presence of Fe_3O_4.

Fe–O bands at 435, 574 and 627 cm^{-1} for the biopolymer-mediated synthesis of magnetite nanoparticles have been reported (Gholoobi et al. 2017). Similarly, a band at 585 cm^{-1} for the *Pisum sativum* peel extract-mediated synthesis of Fe_3O_4 nanoparticles has been mentioned (Prasad et al. 2017). Therefore, the FTIR study revealed the interaction between the alcoholic, amide, carboxylic and amino groups present in the CHLE and the porous CH–Fe_3O_4NPs. In addition, these polyphenolic compounds capped the

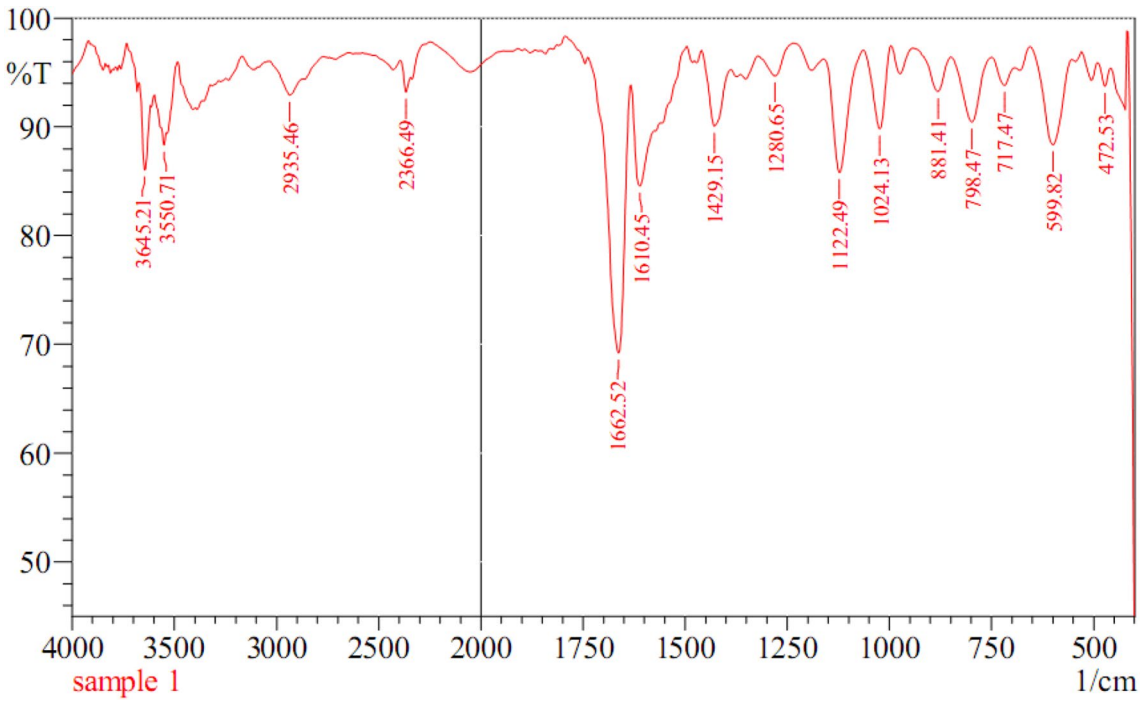

Fig. 6 FTIR spectrum of the CH–Fe_3O_4NPs

Table 2 Comparison of the FTIR data of NPs with standard absorption bands

Bond	Functional group	Frequency range (cm^{-1})	
		Standard	CH–Fe_3O_4NPs
O–H stretch	Alcohols and phenols	3600–3200	3645 and 3550
O–H stretch	Carboxylic acids	3000–2500	2935
C–NH^+ stretch	Charged amines	2500–2325	2366
C=C stretch	Alkenes	1680–1640	1662
N–H bending	Amide II band of proteins	1650–1550	1610
C–H scissoring and bending	Aromatics	1470–1350	1429
C–O stretch	Alcohols, carboxylic acids and esters	1320–1000	1280, 1024 and 1122
C–H bending	Alkenes	1000–675	881, 798 and 717
Fe–O stretch	Iron from iron sulfate	400–600	599 and 472

nanoparticles and rendered stability. The results are consistent with the conclusions made in the SEM analysis with respect to the capping action of polyphenols on the surface of the CH–Fe_3O_4NPs.

Photocatalytic degradation of malachite green dye

The photocatalytic efficacy of the prepared CH–Fe_3O_4NPs was investigated under sunlight irradiation using MG dye as a model pollutant. Figure 7 shows the UV–visible absorbance spectra of 20 ppm MG dye solution with 100 mg of NPs under sunlight irradiation taken at periodic time intervals. The MG dye is characterized by two specific wavelengths namely, 426 nm (associated with aromatic rings) and 617 nm (associated with –C=C– functional group). A continuous decrease in the absorbance spectra of the MG dye solution was observed with the increase in irradiation time. The decrease in the absorbance indicated the decolorization of the dye with the cleavage of chromophore. Under sunlight irradiation, about 67.86% of the dye degraded within 15 min and it became colorless within 55 min. However, the MG dye solution without CH–Fe_3O_4NPs (control) did not show any notable changes in the absorbance and spectrum (data not shown) which validated the importance of the CH–Fe_3O_4NPs for the photocatalytic degradation of the dye.

The degradation kinetics of the dye using CH–Fe_3O_4NPs can be expressed as a pseudo first-order reaction as follows: $\ln C_o/C_f = k_{pd}\, t$.

Herein, k_{pd} is the pseudo first-order photocatalytic degradation rate constant (min^{-1}) which can be calculated from the slope of "$\ln C_o/C_f$ vs t" plot. The value of the k_{pd} was estimated to be 0.0621 min^{-1} and the regression coefficient

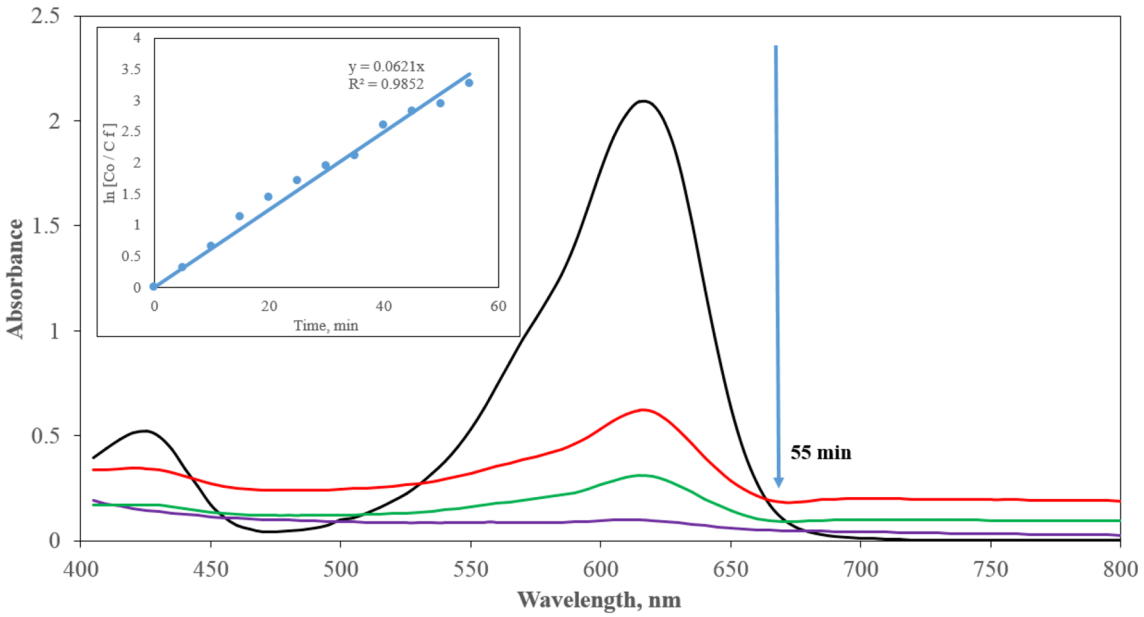

Fig. 7 UV–Vis spectra of MG dye degradation under sunlight irradiation in the presence of CH–Fe_3O_4NPs

(R^2) of 0.9852 (Fig. 7 inset) suggested that the degradation kinetics was well described by pseudo first-order reaction.

It is reported that the reduction of the oxygen and oxidation of water (photocatalytically) on the CH–Fe_3O_4NPs' surface produce highly reactive oxygen species (ROS) which are responsible for the degradation (Kumar et al. 2016). The small size, high surface area and the mesoporous structure (as mentioned in the previous sections) of the CH–Fe_3O_4NPs synthesized in this method effectively degraded the MG dye. This finding is incoherent with the published literature (Muthukumar and Iswarya 2017). In addition, since these CH–Fe_3O_4NPs are magnetic in nature, they can be easily recovered and reused multiple times which decreases the overall process cost.

Conclusions

Mesoporous magnetite nanoparticles have been successfully synthesized using the leaf extract of *Calliandra haematocephala*. The polyphenols of the leaf extract reduced the FeSO4 to form magnetite nanoparticles in a simple, cheap and rapid method without the addition of any other chemicals. The synthesized nanoparticles were characterized by diverse methods such as UV–Vis spectroscopy, SEM, EDS, XRD, FTIR and BET method. The high surface area and mesoporous nature of the synthesized nanoparticles were ascertained from BET analysis. An environmental pollutant dye, Malachite green was rapidly degraded in the presence of the nanoparticles under sunlight radiation which assured the photocatalytic activity. Overall, we conclude that this leaf extract-mediated magnetite nanoparticles may serve as photocatalysts in several environmental applications.

Acknowledgement All the contributors thankfully acknowledge the Department of Biotechnology, Manipal Institute of Technology (MIT), Manipal Academy of Higher Education, for providing all the facilities to perform the research work. Moreover, the authors thankfully acknowledge the timely help and suggestions received from Dr.V.Thivaharan and Dr.V.Ramesh, Associate Professors, Department of Biotechnology, MIT, Manipal Academy of Higher Education, Manipal.

Compliance with ethical standards

Conflict of interests The contributors declare that they do not have any conflict of interests.

References

Balamurugan M (2014) Synthesis of iron oxide nanoparticles by using eucalyptus globulus plant extract. e-Journal Surf Sci Nanotechnol 12(August):363–367

Belachew N, Devi DR, Basavaiah K (2016) Facile green synthesis of L-methionine capped magnetite nanoparticles for adsorption of pollutant Rhodamine B. J Mol Liq 224:713–720

Chauhan N, Narang J, Jain U (2015) Amperometric acetylcholinesterase biosensor for pesticides monitoring utilising iron oxide nanoparticles and poly(indole-5-carboxylic acid). J Exp Nanosci 11(2):111–122

Cheera P, Karlapudi S, Sellola G, Ponneri V (2016) A facile green synthesis of spherical Fe 3 O 4 magnetic nanoparticles and their effect on degradation of methylene blue in aqueous solution. J Mol Liq 221:993–998

Darroudi M, Hakimi M, Goodarzi E, Kazemi Oskuee R (2014) Superparamagnetic iron oxide nanoparticles (SPIONs): green preparation, characterization and their cytotoxicity effects. Ceram Int 40(9):14641–14645

Demir A, Topkaya R, Baykal A (2013) Green synthesis of superparamagnetic Fe_3O_4 nanoparticles with maltose: its magnetic investigation. Polyhedron 65:282–287

Devatha CP, Thalla AK, Katte SY (2016) Green synthesis of iron nanoparticles using different leaf extracts for treatment of domestic waste water. J Clean Prod 139:1425–1435

El Ghandoor H, Zidan HM, Khalil MMH, Ismail MIM (2012) Synthesis and some physical properties of magnetite (Fe_3O_4) nanoparticles. Int J Electrochem Sci 7:5734–5745

Ghanbari D, Salavati-Niasari M, Ghasemi-Kooch M (2014) A sonochemical method for synthesis of Fe_3O_4 nanoparticles and thermal stable PVA-based magnetic nanocomposite. J Ind Eng Chem 20(6):3970–3974

Gholoobi A et al (2017) Biopolymer-mediated synthesis of Fe 3 O 4 nanoparticles and investigation of their in vitro cytotoxicity effects. J Mol Struct 1141:594–599

Guo M, Weng X, Wang T, Chen Z (2017) Biosynthesized iron-based nanoparticles used as a heterogeneous catalyst for the removal of 2,4-dichlorophenol. Sep Purif Technol 175:222–228

Gupta H, Kumar R, Park H-S, Jeon B-H (2017) Photocatalytic efficiency of iron oxide nanoparticles for the degradation of priority pollutant anthracene. Geosyst Eng 20(1):21–27

Hoag GE, Collins JB, Holcomb JL, Hoag JR, Nadagouda MN, Varma RS (2009) Degradation of bromothymol blue by 'greener' nanoscale zero-valent iron synthesized using tea polyphenols. J Mater Chem 19(45):8671

Huang Z, Tang F (2005) Preparation, structure, and magnetic properties of mesoporous magnetite hollow spheres. J Colloid Interface Sci 281(2):432–436

Huang L, Weng X, Chen Z, Megharaj M, Naidu R (2014) Green synthesis of iron nanoparticles by various tea extracts: comparative study of the reactivity. Spectrochim Acta Part A Mol Biomol Spectrosc 130:295–301

Huang L, Luo F, Chen Z, Megharaj M, Naidu R (2015) Green synthesized conditions impacting on the reactivity of Fe NPs for the degradation of malachite green. Spectrochim Acta Part A Mol Biomol Spectrosc 137:154–159

Ibrahim RK, Hayyan M, AlSaadi MA, Hayyan A, Ibrahim S (2016) Environmental application of nanotechnology: air, soil, and water. Environ Sci Pollut Res 23(14):13754–13788

Irshad R, Tahir K, Li B, Ahmad A, Siddiqui AR, Nazir S (2017) Antibacterial activity of biochemically capped iron oxide nanoparticles: a view towards green chemistry. J Photochem Photobiol B Biol 170:241–246

Kumar B, Smita K, Cumbal L, Debut A, Galeas S, Guerrero VH (2016) Phytosynthesis and photocatalytic activity of magnetite (Fe_3O_4) nanoparticles using the Andean blackberry leaf. Mater Chem Phys 179:4–9

Kumari B, Singh DP (2016) A review on multifaceted application of nanoparticles in the field of bioremediation of petroleum hydrocarbons. Ecol Eng 97:98–105

Litvin VA, Minaev BF (2013) Spectroscopy study of silver nanoparticles fabrication using synthetic humic substances and their

antimicrobial activity. Spectrochim Acta Part A Mol Biomol Spectrosc 108:115–122
Litvin VA, Minaev BF (2014) The size-controllable, one-step synthesis and characterization of gold nanoparticles protected by synthetic humic substances. Mater Chem Phys 144(1–2):168–178
Mahdavi M, Namvar F, Bin Ahmad M, Mohamad R (2013) Green biosynthesis and characterization of magnetic iron oxide (Fe_3O_4) nanoparticles using seaweed (Sargassum muticum) aqueous extract. Molecules 18:5954–5964
Mascolo MC, Pei Y, Ring TA (2013) Room temperature co-precipitation synthesis of magnetite nanoparticles in a large ph window with different bases. Materials (Basel) 6(12):5549–5567
Mubarakali D, Thajuddin N, Jeganathan K, Gunasekaran M (2011) Plant extract mediated synthesis of silver and gold nanoparticles and its antibacterial activity against clinically isolated pathogens. Colloids Surf B Biointerfaces 85(2):360–365
Muthukumar H, Iswarya N (2017) Iron oxide nano-material: physico-chemical traits and in vitro antibacterial propensity against multidrug resistant bacteria. J Ind Eng Chem 45:121–130
Muthukumar Harshiny, Matheswaran Manickam (2015) Amaranthus spinosus leaf extract mediated FeO nanoparticles: physicochemical traits, photocatalytic and antioxidant activity. ACS Sustain Chem Eng 3(12):3149–3156
Nabiyouni G, Julaee M, Ghanbari D, Aliabadi PC, Safaie N (2015) Room temperature synthesis and magnetic property studies of Fe_3O_4 nanoparticles prepared by a simple precipitation method. J Ind Eng Chem 21:599–603
Peralta-videa JR, Huang Y, Parsons JG, Zhao L (2016) Plant-based green synthesis of metallic nanoparticles: scientific curiosity or a realistic alternative to chemical synthesis? Nanotechnol Environ Eng 1(1):1–29
Prasad C, Yuvaraja G, Venkateswarlu P (2017) Biogenic synthesis of Fe_3O_4 magnetic nanoparticles using Pisum sativum peels extract and its effect on magnetic and Methyl orange dye degradation studies. J Magn Magn Mater 424:376–381
Raja S, Ramesh V, Thivaharan V (2017) Green biosynthesis of silver nanoparticles using Calliandra haematocephala leaf extract, their antibacterial activity and hydrogen peroxide sensing capability. Arab J Chem 10(2):253–261
Ren G, Yang L, Zhang Z, Zhong B, Yang X, Wang X (2017) A new green synthesis of porous magnetite nanoparticles from waste ferrous sulfate by solid-phase reduction reaction. J Alloys Compd 710:875–879
Shaofeng Z, Wei W, Xiangheng X, Juan Z, Feng R, Changzhong Jiang (2011) Preparation and characterization of spindle-like Fe_3O_4 mesoporous nanoparticles. Nanoscale Res Lett 6:89–97
Siddiqi KS, ur Rahman A, Tajuddin, Husen A (2016) Biogenic fabrication of iron/iron oxide nanoparticles and their application. Nanoscale Res Lett 11(1):498
Smuleac V, Varma R, Sikdar S, Bhattacharyya D (2011) Green synthesis of Fe and Fe/Pd bimetallic nanoparticles in membranes for reductive degradation of chlorinated organics. J Membr Sci 379(1–2):131–137
Stan M et al (2017) Removal of antibiotics from aqueous solutions by green synthesized magnetite nanoparticles with selected agro-waste extracts. Process Saf Environ Prot 107:357–372
Taha MR, Ibrahim AH (2014) Characterization of nano zero-valent iron (nZVI) and its application in sono-Fenton process to remove COD in palm oil mill effluent. J Environ Chem Eng 2(1):1–8
Venkateswarlu S, Rao YS, Balaji T, Prathima B, Jyothi NVV (2013) Biogenic synthesis of Fe_3O_4 magnetic nanoparticles using plantain peel extract. Mater Lett 100:241–244
Venkateswarlu S, Natesh Kumar B, Prasad CH, Venkateswarlu P, Jyothi NVV (2014a) Bio-inspired green synthesis of Fe_3O_4 spherical magnetic nanoparticles using Syzygium cumini seed extract. Phys B Condens Matter 449:61–71
Venkateswarlu S, Kumar BN, Prathima B, SubbaRao Y, Jyothi NVV (2014b) A novel green synthesis of Fe_3O_4 magnetic nanorods using Punica Granatum rind extract and its application for removal of Pb(II) from aqueous environment. Arab J Chem. https://doi.org/10.1016/j.arabjc.2014.09.006
Wang T, Lin J, Chen Z, Megharaj M, Naidu R (2014) Green synthesized iron nanoparticles by green tea and eucalyptus leaves extracts used for removal of nitrate in aqueous solution. J Clean Prod 83:413–419
Wang J, Liu G, Liu Y, Zhou C, Wu Y (2017) Photocatalytic degradation of methyl orange by Fe_2O_3–Fe_3O_4 nanoparticles and Fe_2O_3–Fe_3O_4–montmorillonite nanocomposites. Clean Soil Air Water 45(9):1600472
Xu P et al (2014) Photocatalytic degradation of phenol by the heterogeneous Fe_3O_4 nanoparticles and oxalate complex system. RSC Adv 4(77):40828–40836
Zazouli MA, Ghanbari F, Yousefi M, Madihi-Bidgoli S (2017) Photocatalytic degradation of food dye by Fe_3O_4–TiO2 nanoparticles in presence of peroxymonosulfate: the effect of UV sources. J Environ Chem Eng 5(3):2459–2468